Catalysis Today 161 (2011) 163–168

Contents lists available at ScienceDirect

Catalysis Today

journal homepage: www.elsevier.com/locate/cattod

Kinetics of UV-A/TiO_2 photocatalytic degradation and mineralization of the antibiotic sulfamethoxazole in aqueous matrices

Nikolaos P. Xekoukoulotakis[a,*], Catherine Drosou[a], Christina Brebou[a], Efthalia Chatzisymeon[a], Evroula Hapeshi[b], Despo Fatta-Kassinos[b], Dionissios Mantzavinos[a,**]

[a] Department of Environmental Engineering, Technical University of Crete, University Campus, Polytechneioupolis, GR-73100 Chania, Crete, Greece
[b] Department of Civil and Environmental Engineering, University of Cyprus, 75 Kallipoleos St., 1678 Nicosia, Cyprus

ARTICLE INFO

Article history:
Available online 28 October 2010

Keywords:
Sulfamethoxazole
Kinetics
Photocatalysis
TiO_2
Water

ABSTRACT

The photocatalytic degradation and mineralization of the antibiotic sulfamethoxazole (SMX) in aqueous TiO_2 suspensions was investigated. UV-A irradiation was provided by a 9 W lamp at a photon flux of 2.81×10^{-4} Einstein/min and runs were performed at SMX initial concentrations between 2.5 and 30 mg/L, six commercially available TiO_2 catalysts at loadings between 100 and 750 mg/L, acidic or near-neutral conditions and three different water matrices. Of the various catalysts tested, Degussa P25 was highly active, i.e. nearly complete SMX degradation and mineralization could be achieved after 30 and 120 min of reaction, respectively at 10 mg/L SMX and 250 mg/L catalyst concentrations. SMX and organic carbon conversion decreased with decreasing titania loading and dissolved oxygen concentration and increasing SMX concentration and solution pH. The presence of non-target constituents in environmental samples only marginally affected SMX degradation. For the range of concentrations studied, a Langmuir–Hinshelwood kinetic model can describe the process.

1. Introduction

The occurrence of pharmaceuticals and their metabolites and transformation products in the environment is becoming a matter of concern because these compounds, which may have adverse effects on living organisms, are extensively and increasingly used in human and veterinary medicine and are released continuously into the environment [1,2]. A variety of pharmaceuticals have been detected in many environmental samples worldwide. Their occurrence has been reported in wastewater treatment plant effluents, surface water, seawater, groundwater, soils and sediments and is closely related to their bioresistant nature [3,4].

Among the various pharmaceutical compounds present in the environment, special emphasis has been given to antibiotics, which are the most often discussed pharmaceuticals because of their potential role in the development of antibiotic-resistant bacteria [5]. Antibiotics are used extensively in human and veterinary medicine, as well as in aquaculture, for the purpose of preventing or treating microbial infections. They are often partially metabolized in the organism (i.e. less than 30%) and they are excreted as the parent substance or as metabolites into wastewaters at concentrations ranging from ng/L to μg/L [6].

Most antibiotics tested to date are known to be biorecalcitrant under aerobic conditions [6], thus escaping intact from conventional wastewater treatment plants. In this perspective, non-biological methods such as advanced oxidation processes (AOPs) have been employed to treat pharmaceuticals and alike xenobiotics in various aqueous matrices and representative studies have been thoroughly reviewed recently [7]. These processes are characterized by the formation of hydroxyl radicals, which exhibit high reactivity and efficiency in oxidizing a great variety of organic micro-pollutants, including pharmaceuticals.

Sulfamethoxazole (SMX) is a synthetic antibiotic and belongs to the group of sulfonamide antibiotics. It is the most commonly employed antibiotic of this group and it is extensively used in both human and veterinary medicine. There have been a few recent studies dealing with SMX advanced oxidation by means of ozonation [8–10], anodic oxidation over boron-doped diamond electrodes [11,12], oxidation with free chlorine and monochloramine [13] and modified Fenton reaction [14]. Particular emphasis has recently been given on photochemical AOPs such as (i) homogeneous Fenton oxidation induced by solar [15–18] or artificial [17,19] light and coupled with biological post-treatment [20], and (ii) semiconductor photocatalysis [21–25]. Abellan et al. [21,22] and Bayarri et al. [23] investigated the effect of TiO_2 concentration and light wavelength, respectively on the kinetics of SMX degradation and mineralization

* Corresponding author. Tel.: +30 2821037796; fax: +30 2821035852.
** Corresponding author. Tel.: +30 2821037797; fax: +30 2821035852.
E-mail addresses: nikos.xekoukoulotaki@enveng.tuc.gr (N.P. Xekoukoulotakis), mantzavi@mred.tuc.gr (D. Mantzavinos).

0920-5861/$ – see front matter © 2010 Elsevier B.V. All rights reserved.
doi:10.1016/j.cattod.2010.09.027

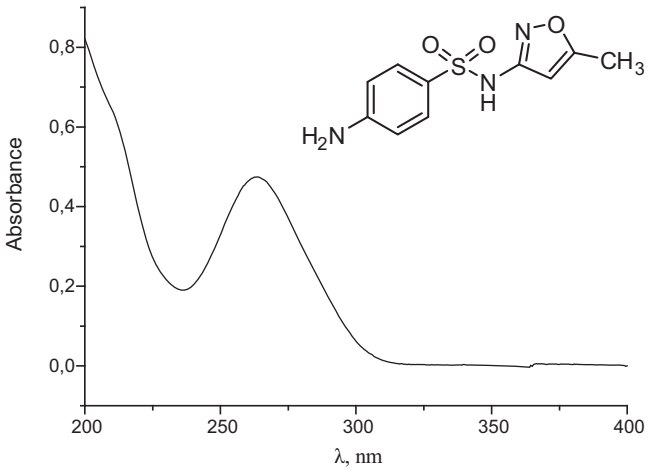

Scheme 1. The molecular structure and absorbance spectrum of SMX.

under simulated solar conditions, while Baran et al. [24] compared the efficiency of UV-A/TiO_2, UV-A/Fe^{3+} and UV-A/TiO_2/Fe^{3+} systems for the degradation and mineralization of five sulfa drugs including SMX. In their studies, Abellan et al. [22] and Hu et al. [25] identified several intermediates accompanying SMX photocatalytic degradation and proposed respective reaction pathways.

The aim of this work was to study, in a systematic way, the effect of various process parameters such as TiO_2 type and loading, initial antibiotic concentration, solution pH, the presence of electron acceptors and the water matrix (i.e. ultrapure water, groundwater and treated wastewater) on the kinetics of SMX degradation and mineralization under UV-A irradiation; such a methodical approach has only merely been reported in the literature.

2. Materials and methods

2.1. Materials

SMX ($C_{10}H_{11}N_3O_3S$, molecular mass 253.28 g/mol, shown in Scheme 1) was purchased from Sigma (CAS 723-46-6) and used as received. In most cases, ultrapure water (UPW) taken from a water purification system (EASYpureRF - Barnstead/Thermolyne, USA) was used to prepare SMX solutions; in certain cases though, groundwater (GW) taken from a pumping well and the treated effluent (WW) from the central municipal wastewater treatment plant of Limassol, Cyprus, were also spiked with SMX to assess the effect of water matrix on degradation. The quality characteristics of the GW and WW are given in detail elsewhere [26]. Six commercially available TiO_2 samples, whose main properties are summarized in Table 1, were employed for slurry photocatalytic experiments.

2.2. Experimental procedure

UV-A irradiation was provided by a 9 W lamp (Radium Ralutec, 9W/78) emitting predominantly at 350–400 nm. The photon flux emitted from the lamp was determined actinometrically using the potassium ferrioxalate method and was found 2.81×10^{-4} Einstein/min. Experiments were conducted in an immersion well, batch type, laboratory scale photoreactor, purchased from Ace Glass (Vineland, NJ, USA) and described in detail elsewhere [27].

In a typical photocatalytic run, 350 mL of the aqueous solution containing the desired concentration of SMX in the range 2.5–30 mg/L were loaded in the reaction vessel. These concentrations, although considerably greater than those typically found in environmental samples, were chosen to allow (i) the assessment of process efficiency within a measurable time scale, and (ii) the accurate determination of residual SMX and organic carbon with the analytical techniques employed in this work. The solution was slurried with the appropriate amount of catalyst and magnetically stirred for 30 min in the dark to ensure complete equilibration of adsorption/desorption of SMX onto the TiO_2 surface. After that period, the UV-A lamp was turned on, while pure O_2 was continuously sparged (unless otherwise stated) in the reaction mixture under stirring. During photocatalytic experiments, temperature was maintained at 25 °C with a temperature control unit. Most experiments were performed at inherent solution pH which was left uncontrolled during the reaction; the inherent solution pH was acidic (the exact value was dependent of SMX initial concentration and the type of catalyst) at UPW and near-neutral/slightly alkaline at GW or WW. For those runs where the initial pH had to be adjusted, this was done adding the appropriate amount of 0.5N NaOH or 0.5N HCl solutions, as necessary. Photocatalytic experiments were performed in several replicates (i.e. between 2 and 6) and mean values, whose standard deviation never exceeded 5%, are quoted as results.

2.3. Analytical techniques

Samples periodically taken from the reactor were centrifuged at 13,200 rpm to remove catalyst particles and then analyzed for (i) total organic carbon (TOC) content, as described elsewhere [28], and (ii) residual SMX concentration. The latter was followed by high performance liquid chromatography (Agilent 1100 series HPLC) employing a Supelco C-18 column (5 μm, 4.6 mm × 150 mm) and a diode array detector set at 266 nm. A 60:40 acidified water (pH of about 3) and acetonitrile mixture was employed as the mobile phase at a flow rate of 1 mL/min and a constant temperature of 20 °C.

3. Results and discussion

3.1. Catalyst screening and activity

To assess the relative catalytic activity of various TiO_2 samples, preliminary experiments were conducted at 10 mg/L SMX initial concentration, 250 mg/L catalyst loading and inherent solution pH of 4.1–5.4 depending on the type of catalyst. Fig. 1a shows that Degussa P25 is considerably more active than all other TiO_2 samples leading to nearly complete SMX disappearance after 30 min of reaction; the respective conversion for the rest does not exceed

Table 1
TiO_2 catalysts used in this study. A: anatase; R: rutile.

Catalyst	Crystal form	BET area, m^2/g	Particle size, nm	Supplier
Degussa P25	75%A:25%R	50	21	Degussa AG
Hombikat UV 100	A > 99%	<250	5	Sachtleben Chemie GmbH
Millennium PC 50	A > 97%	45–55	20–30	Millennium Inorganic Chemicals
Millennium PC 100	A > 95%	80–100	15–25	Millennium Inorganic Chemicals
Millennium PC 105	A > 95%	75–95	15–25	Millennium Inorganic Chemicals
Millennium PC 500	A > 75%	<300	5–10	Millennium Inorganic Chemicals

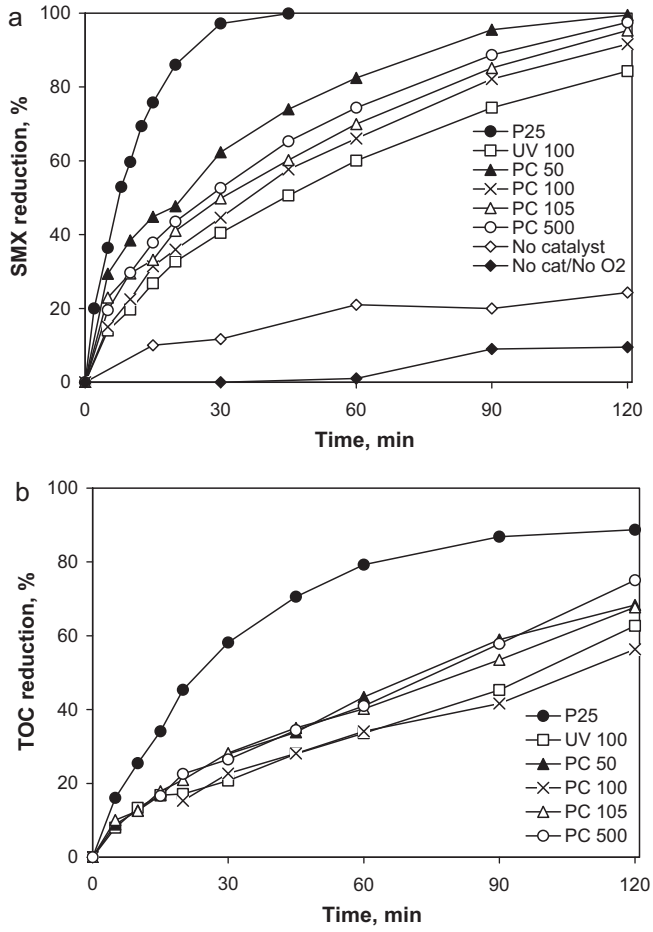

Fig. 1. Relative activity of various TiO_2 samples (250 mg/L) for 10 mg/L SMX (a) degradation and (b) mineralization.

65%. Similarly, mineralization is favored in the presence of Degussa P25 reaching about 90% after 120 min (Fig. 1b). The greater activity of Degussa P25 is particularly notable taking into account that its surface area is lower (with the exception of Millennium PC 50) than the rest. These results are in good agreement with the work of Hu et al. [25] who reported that Degussa P25 was far more active than Hombikat UV 100 for SMX degradation under UV-A irradiation.

The superiority of Degussa P25 is attributed [29,30] to the slower electron/hole recombination taking place on the catalyst surface compared to other TiO_2 photocatalysts; another explanation ascribes the higher activity of Degussa P25 to its structure which is a mixture of anatase and rutile; this mixture is more active than the individual pure crystalline phases [31]. According to the above findings, all subsequent photocatalytic experiments were performed with Degussa P25 TiO_2.

To confirm that SMX degradation is due to the synergy between photonic energy and the catalyst surface, an additional experiment was performed in the absence of catalyst. As seen in Fig. 1a, the extent of SMX conversion did not exceed 20% after 120 min and this is believed to be due to photooxidation involving dissolved oxygen rather than photolysis; the latter is unlikely to occur at the conditions in question since the absorbance spectrum of SMX (Scheme 1) fades out at about 305 nm, i.e. well below the emission spectrum of the irradiation source. At the same time, TOC reduction was inconsiderable (data not shown). The experiment was repeated without oxygen sparging and this led to 10% SMX conversion after 120 min confirming the above hypothesis (although some dissolved oxygen is still present due to agitation). Dark adsorption experiments were

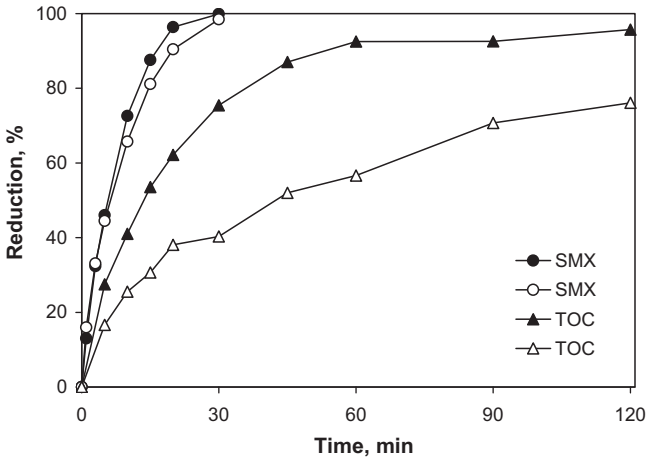

Fig. 2. Effect of oxygen sparging on 10 mg/L SMX degradation and mineralization with 500 mg/L Degussa P25. Closed and open symbols show runs with and without oxygen sparging, respectively.

also performed at 500 mg/L Degussa P25 concentration; in all cases (i.e. 2.5 or 10 mg/L SMX concentration, inherent or near-neutral pH), SMX adsorption remained below 5%.

3.2. Effect of dissolved oxygen

The presence of dissolved oxygen in the liquid phase is expected to enhance photocatalytic oxidation since oxygen traps the photogenerated conduction band electrons to form superoxide radical anions as follows:

$$e^-_{CB} + O_2 \rightarrow O_2^{\bullet -} \quad (1)$$

Reaction (1) is critical to the photocatalytic performance for two reasons, namely: (i) the undesirable recombination of electrons and valence band holes is minimized, and (ii) more reactive oxygen species are formed since superoxide radical anions may react with protons formed through water splitting to yield peroxide radicals.

Fig. 2 shows a comparison between runs performed under conditions of limited (i.e. no aeration takes place but the reactor is open to the air) and excessive (i.e. continuous oxygen supply occurs) dissolved oxygen. An excess of oxygen has a beneficial effect on mineralization (e.g. the extent of TOC reduction is 96% and 76% after 120 min with and without aeration, respectively) but it only marginally affects SMX degradation. Partial oxidation reactions (i.e. SMX conversion to intermediates) typically occur at greater rates than total oxidation reactions (i.e. mineralization of deep oxidation intermediates) and this explains the different degree of oxygen effect on the process. In addition, there is a possibility that the partial oxidation of SMX might have resulted in the formation of volatile intermediate oxidation products, which could have been stripped by the oxygen stream. This could potentially explain, at least in part, the reduced mineralization rate of SMX under continuous oxygen supply. However, this has not been investigated in the framework of the present work.

3.3. Effect of SMX concentration

The effect of varying SMX initial concentration was studied in the range 2.5–30 mg/L at 500 mg/L Degussa P25 loading and the results are shown in Fig. 3a, while Table 2 summarizes the initial reaction rates for SMX degradation and TOC removal, calculated over the first 5 min and 10 min of reaction, respectively. As seen, the initial reaction rate for SMX photocatalytic degradation increases from 0.428 mg/(L × min) to 1.510 mg/(L × min) by increasing SMX

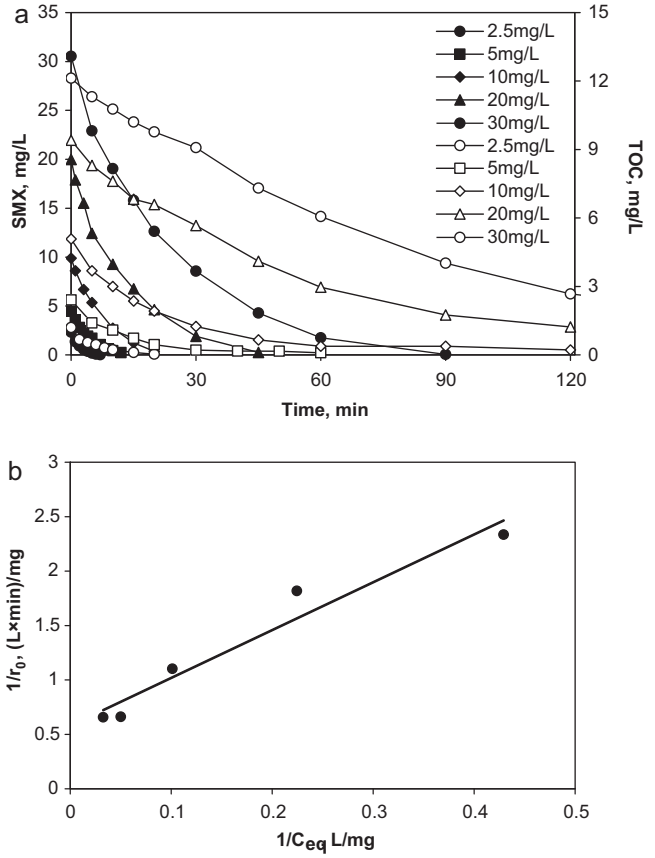

Fig. 3. (a) Effect of initial SMX concentration on degradation and mineralization with 500 mg/L Degussa P25. Closed and open symbols refer to SMX (left axis) and TOC (right axis) temporal profiles, respectively and (b) the L–H kinetic model for SMX degradation.

initial concentration from 2.5 mg/L to 20 mg/L, respectively, while at higher SMX initial concentration (i.e. 30 mg/L) the initial reaction rate for SMX degradation levels off. On the other hand, the initial reaction rate for TOC removal increases from 0.097 mg/(L × min) to 0.208 mg/(L × min) by increasing SMX initial concentration from 2.5 mg/L to 10 mg/L, respectively, while further increase of SMX initial concentration results in decreasing the initial reaction rate for TOC removal. In addition, mineralization was 4–11 times slower than SMX degradation, thus indicating the formation of difficult to degrade reaction intermediates that tend to remain in the liquid phase and have a negative effect on the rate of mineralization.

The above results on the photocatalytic degradation of SMX can be explained in terms of the Langmuir–Hinshelwood (L–H) kinetic model [32,33], i.e.

$$r_0 = k_r \frac{KC_{eq}}{1 + KC_{eq}} \Leftrightarrow \frac{1}{r_0} = \frac{1}{k_r K}\frac{1}{C_{eq}} + \frac{1}{k_r} \quad (2)$$

where r_0 is the initial reaction rate for SMX photocatalytic degradation, C_{eq} is the equilibrium SMX concentration, K is the adsorption constant of SMX onto the catalyst surface and k_r is the intrinsic reaction rate constant for SMX degradation. A plot of the linearized form of Eq. (2) is shown in Fig. 3b. The L–H model-derived values for k_r and K are 1.73 mg/(L × min) and 0.13 L/mg, respectively. Similar values (k_r = 1.91 mg/(L × min) and K = 0.17 L/mg) were reported by Hu et al. [25] who studied SMX degradation under UV-A irradiation at 9×10^{-5} Einstein/min, 100 mg/L Degussa P25, 1.1–121 mg/L initial SMX concentration and at pH = 3. Notably, the derived K value is greater than expected since the extent of dark adsorption is very low; this has also been reported by several other investigators [25] and is attributed to enhanced photo-adsorption, i.e. UV-A irradiation is believed to alter catalyst surface properties in a way that facilitates substrate adsorption.

In addition, the quantum yield, Φ, was calculated for the photocatalytic degradation of SMX and for TOC removal according to Eq. (3), and the results are also shown in Table 2.

$$\Phi = \frac{r_0}{I/V} \times 100 \quad (3)$$

where r_0 is the initial reaction rate for SMX photocatalytic degradation and TOC removal expressed in mol/(L × min), I is the incident photon flux (i.e. 2.81×10^{-4} Einstein/min) and V is the volume of the reactor (i.e. 0.35 L).

As can be seen, at the conditions employed in the present study, the quantum yield ranged from 0.21% to 0.75% for the photocatalytic degradation of SMX, and from 0.92% to 2.15% for TOC removal.

3.4. Effect of catalyst loading

The effect of catalyst loading on 10 mg/L SMX degradation and mineralization was studied in the range 100–750 mg/L and inherent solution pH and the results are shown in Fig. 4 and Table 2. As seen, reaction rates increase with increasing catalyst concentration up to 500 mg/L after which they remain practically unchanged. The increase in photocatalytic activity with increasing catalyst loading indicates a heterogeneous catalytic regime since the fraction of incident light absorbed by the semiconductor progressively increases in suspensions containing higher amounts of TiO_2 [21]. However, photocatalytic activity reached a plateau at about 500 mg/L TiO_2

Table 2
Kinetics of SMX degradation and mineralization at different conditions under oxygen sparging. The initial reaction rates for SMX degradation, $r_{0\,SMX}$, were calculated over the first 5 min of reaction, while the initial reaction rates for TOC removal, $r_{0\,TOC}$, were calculated over the first 10 min of reaction. The quantum yield, Φ, for SMX degradation and TOC removal was calculated according to Eq. (3). UPW: ultrapure water; GW: groundwater; WW: treated wastewater; ND: not determined.

SMX, mg/L	Degussa P25, mg/L	Water matrix	pH_o	SMX degradation		TOC removal	
				$r_{0\,SMX}$, mg/(L × min)	Φ, %	$r_{0\,TOC}$, mg/(L × min)	Φ, %
2.5	500	UPW	4 ± 0.1	0.428	0.21	0.097	1.01
5	500	UPW	4 ± 0.1	0.550	0.27	0.132	1.37
10	500	UPW	4 ± 0.1	0.906	0.45	0.208	2.15
20	500	UPW	4 ± 0.1	1.510	0.74	0.180	1.86
30	500	UPW	4 ± 0.1	1.522	0.75	0.136	1.40
10	100	UPW	4 ± 0.1	0.769	0.38	0.089	0.92
10	250	UPW	4 ± 0.1	0.775	0.38	0.130	1.35
10	750	UPW	4 ± 0.1	0.879	0.43	0.182	1.88
10	500	UPW	7.5 ± 0.3	0.866	0.43	0.099	1.03
10	500	GW	5.2 ± 0.4	0.873	0.43	ND	ND
10	500	GW	8 ± 0.2	0.559	0.27	ND	ND
10	500	WW	5.2 ± 0.4	0.900	0.44	ND	ND
10	500	WW	7.9 ± 0.3	0.593	0.29	ND	ND

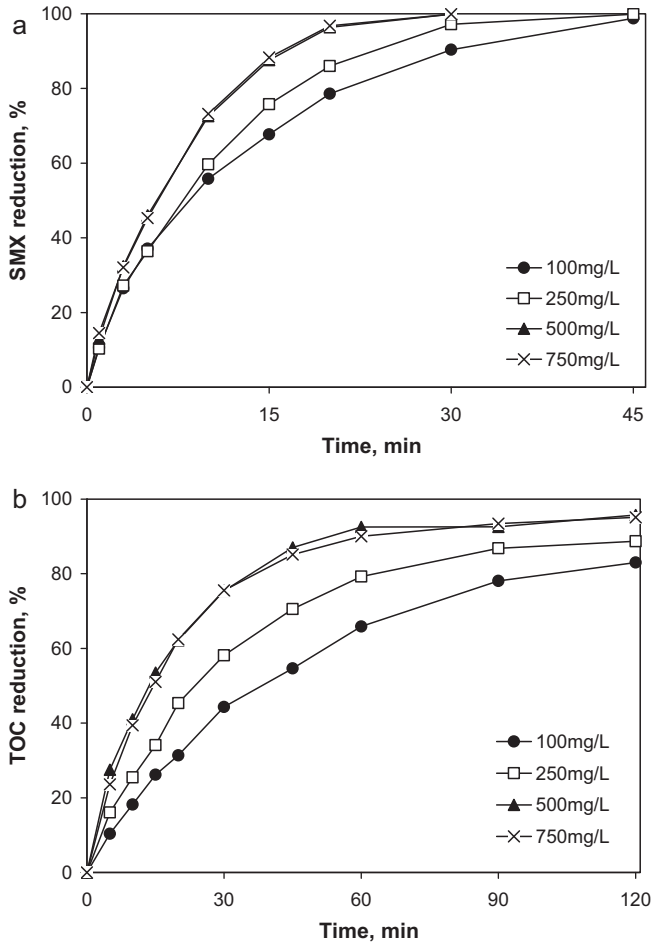

Fig. 4. Effect of Degussa P25 loading on 10 mg/L SMX (a) degradation and (b) mineralization.

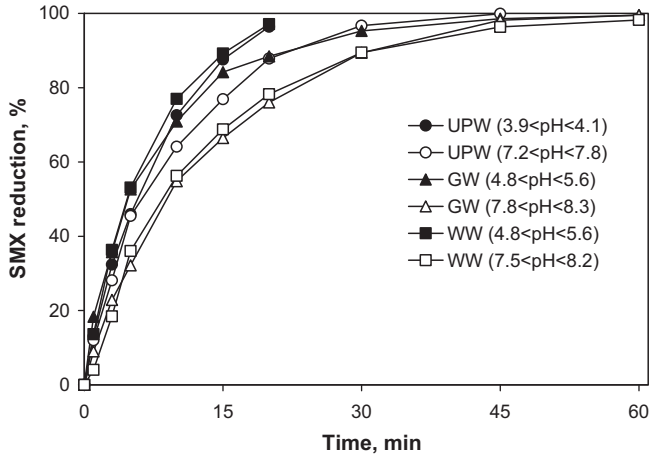

Fig. 5. Effect of initial solution pH and water matrix on 10 mg/L SMX degradation with 500 mg/L Degussa P25.

loading. The catalyst concentration above which conversion levels off depends on several factors (e.g. reactor geometry, substrate concentration, wavelength and intensity of light source) and corresponds to the point where all catalyst particles, i.e. all the surface exposed, are fully illuminated [32]. At higher concentrations, a screening effect of excess particles occurs, thus masking part of the photosensitive surface and consequently hindering light penetration; this usually results in conversion reaching a plateau, while at excessive catalyst concentrations conversion may also decrease due to increased light reflectance onto the catalyst surface.

3.5. *Effect of initial solution pH and the water matrix*

Fig. 5 and Table 2 show the effect of water matrix and the initial solution pH on 10 mg/L SMX degradation at 500 mg/L Degussa P25. Experiments with actual environmental samples showed that the presence of about 10 mg/L effluent organic matter (measured as TOC) in WW had practically little effect on degradation and so did the presence of about 2 mg/L TOC and 220 mg/L of bicarbonates (i.e. known scavengers of hydroxyl radicals and other reactive moieties) in GW compared to UPW at the same pH conditions. In this sense, the non-target constituents typically found in environmental samples do not impede the photocatalytic degradation of the target compound at the conditions in question.

Regardless the water matrix involved, degradation is favored at acidic conditions but decreases at near-neutral/slightly alkaline pH, and this was more pronounced at GW and WW matrixes. A possible explanation might be given in terms of (i) the effect of solution pH on the photo-adsorption of SMX onto the catalyst surface, which is an important step for the photocatalytic oxidation to take place [33] and (ii) the effect of pH and ionic strength on the agglomeration of TiO_2 particles in aquatic suspensions.

More specifically, the SMX molecule contains one basic amine group ($-NH_2$) and one acidic amide group (–NH–) and therefore it has two pK_a values, namely p$K_{a,1} = 1.85 \pm 0.30$ and p$K_{a,2} = 5.60 \pm 0.04$ [34,35]. The acid-base dissociation equilibrium of SMX is illustrated in Fig. 6. The amine group is able to gain a proton, while the amide group is able to release a proton under specific pH conditions. As shown in Fig. 6, $K_{a,1}$ is the dissociation constant for the equilibrium between the positively charged, protonated amino group of SMX and its electrically neutral conjugate base, while $K_{a,2}$ refers to the equilibrium involving the loss of the sulfonamide proton to yield its negatively charged conjugate base. Therefore, at pH values below p$K_{a,1}$ and above p$K_{a,2}$ the positively and negatively charged forms of SMX prevail, respectively, while at pH values between p$K_{a,1}$ and p$K_{a,2}$ SMX exists predominately in its neutral form. On the other hand, at pH values lower than about 6.7, which is the point of zero charge for Degussa P25 TiO_2 [36], the TiO_2 surface becomes positively charged, while at pH values greater than about 6.7 it becomes negatively charged. Therefore, at near-neutral/slightly alkaline pH both SMX and the catalyst surface are negatively charged and the repulsion between them is enhanced, and therefore the photo-adsorption of SMX onto the catalyst surface is expected to be reduced. This may explain, in part, the decreased photocatalytic activity observed at near-neutral/slightly alkaline pH.

In addition, it is well known that TiO_2 particles tend to form agglomerates when dispersed in aqueous media, and such agglomeration is strongly depended on parameters such as ionic strength and pH of the suspension [37,38]. Recently, it has been reported that Degussa P25 TiO_2 particles agglomeration in aquatic suspensions decreases at acidic conditions compared to neutral conditions [37], thus increasing the effective surface area of the photocatalyst in the aqueous suspension. This increase of the effective surface area of the photocatalyst at acidic condition can also explain, in part, the increased photocatalytic activity for the degradation of SMX at acidic conditions.

Moreover, it has been reported that increasing the ionic strength of the solution results in increased TiO_2 particles agglomeration [38], thus decreasing the effective surface area of the photocatalyst. This finding can explain our observation that the photocatalytic degradation of SMX was reduced in a grater extent going from acidic to near-neutral/slightly alkaline pH at GW and WW matrixes com-

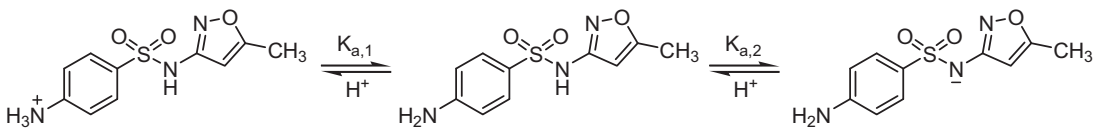

Fig. 6. Acid–base dissociation equilibrium of SMX.

pared to UPW, because the former matrixes (i.e. GW and WW) have larger ionic strengths than UPW and consequently TiO_2 particles tend to form larger agglomerates in GW and WW and thus having lower effective surface area.

4. Conclusions

The conclusions drawn from the present study can be summarized as follows:

(1) Semiconductor photocatalysis based on Degussa P25 TiO_2 is an efficient method for the degradation and mineralization of sulfamethoxazole in aqueous solutions. Process performance is affected by several factors, namely irradiation time, photocatalyst type and loading, the presence of electron acceptors and the solution pH.
(2) The degradation can be represented by a Langmuir–Hinshelwood (L–H) kinetic model. Higher sulfamethoxazole and TOC conversions are achieved at lower concentrations. Since the levels of sulfamethoxazole and alike compounds in environmental samples are relatively low (e.g. 2–3 orders of magnitude lower than those employed in this work), their degradation is likely to occur readily at mild operating conditions.

Acknowledgement

The authors are grateful to the Cyprus Research Promotion Foundation for funding this research project (PHAREM-AEIFO/0506/16).

References

[1] T.A. Ternes, A. Joss, Human Pharmaceuticals, Hormones and Fragrances: The Challenge of Micropollutants in Urban Water Management, first ed., IWA, Cornwall, 2006.
[2] K. Kümmerer, Pharmaceuticals in the Environment: Sources, Fate, Effects and Risks, third ed., Springer, Berlin, 2008.
[3] D. Fatta-Kassinos, K. Bester, K. Kümmerer, Xenobiotics in the urban water cycle: mass flows, environmental processes, mitigation and treatment strategies Environmental Pollution, Vol. 16, Springer, 2010.
[4] A. Nikolaou, S. Meric, D. Fatta, Anal. Bioanal. Chem. 387 (2007) 1225–1234.
[5] K. Kümmerer, Chemosphere 75 (2009) 435–441.
[6] K. Kümmerer, Chemosphere 75 (2009) 417–434.
[7] M. Klavarioti, D. Mantzavinos, D. Kassinos, Environ. Int. 35 (2009) 402–417.
[8] A.Y.C. Lin, C.F. Lin, J.M. Chiou, P.K.A. Hong, J. Hazard. Mater. 171 (2009) 452–458.
[9] F.J. Beltran, A. Aguinaco, J.F. Garcia-Araya, Water Res. 43 (2009) 1359–1369.
[10] R.F. Dantas, S. Contreras, C. Sans, S. Esplugas, J. Hazard. Mater. 150 (2008) 790–794.
[11] J. Boudreau, D. Bejan, S. Li, N.J. Bunce, Ind. Eng. Chem. Res. 49 (2010) 2537–2542.
[12] S. Li, D. Bejan, M.S. McDowell, N.J. Bunce, J. Appl. Electrochem. 38 (2008) 151–159.
[13] E. Chamberlain, C. Adams, Water Res. 40 (2006) 2517–2526.
[14] D. Marciocha, J. Kalka, J. Turek-Szytow, J. Wiszniowski, J. Surmacz-Gorska, Water Sci. Technol. 60 (2009) 2555–2562.
[15] N. Klamerth, L. Rizzo, S. Malato, M.I. Maldonado, A. Aguera, A.R. Fernandez-Alba, Water Res. 44 (2010) 545–554.
[16] A.G. Trovo, R.F.P. Nogueira, A. Aguera, A.R. Fernandez-Alba, C. Sirtori, S. Malato, Water Res. 43 (2009) 3922–3931.
[17] O. Gonzalez, C. Sans, S. Esplugas, S. Malato, Photochem. Photobiol. Sci. 8 (2009) 1032–1039.
[18] N. Klamerth, N. Miranda, S. Malato, A. Aguera, A.R. Fernandez-Alba, M.I. Maldonado, J.M. Coronado, Catal. Today 144 (2009) 124–130.
[19] O. Gonzalez, C. Sans, S. Esplugas, J. Hazard. Mater. 146 (2007) 459–464.
[20] O. Gonzalez, M. Esplugas, C. Sans, S. Esplugas, Water Sci. Technol. 58 (2008) 1707–1713.
[21] M.N. Abellan, J. Gimenez, S. Esplugas, Catal. Today 144 (2009) 131–136.
[22] M.N. Abellan, B. Bayarri, J. Gimenez, J. Costa, Appl. Catal. B: Environ. 74 (2007) 233–241.
[23] B. Bayarri, M.N. Abellan, J. Gimenez, S. Esplugas, Catal. Today 129 (2007) 231–239.
[24] W. Baran, E. Adamek, A. Sobczak, A. Makowski, Appl. Catal. B: Environ. 90 (2009) 516–525.
[25] L. Hu, P.M. Flanders, P.L. Miller, T.J. Strathmann, Water Res. 41 (2007) 2612–2626.
[26] E. Hapeshi, A. Achilleos, M.I. Vasquez, C. Michael, N.P. Xekoukoulotakis, D. Mantzavinos, D. Kassinos, Water Res. 44 (2010) 1737–1746.
[27] C. Fotiadis, N.P. Xekoukoulotakis, D. Mantzavinos, Catal. Today 124 (2007) 247–253.
[28] N.P. Xekoukoulotakis, N. Xinidis, M. Chroni, D. Mantzavinos, D. Venieri, E. Hapeshi, D. Fatta-Kassinos, Catal. Today 151 (2010) 29–33.
[29] S.T. Martin, H. Herrmann, W. Choi, M.R. Hoffmann, J. Chem. Soc., Faraday Trans. 21 (1994) 3315–3322.
[30] C.A. Emilio, M.I. Litter, K. Marinus, M. Bouchard, C. Colbeau-Justin, Langmuir 22 (2006) 3606–3613.
[31] R.I. Bickley, T. Gonzalez-Carreno, J.S. Lees, L. Palmisano, R.J.D. Tilley, J. Solid State Chem. 92 (1991) 178–190.
[32] J.-M. Herrmann, Appl. Catal. B: Environ. 99 (2010) 461–468.
[33] D. Friedmann, C. Mendive, D. Bahnemann, Appl. Catal. B: Environ. 99 (2010) 398–406.
[34] Z. Qiang, C. Adams, Water Res. 38 (2004) 2874–2890.
[35] S. Babić, A.J.M. Horvat, D. Mutavdžić Pavlović, M. Kaštelan-Macan, Trac-Trends Anal. Chem. 26 (2007) 1043–1061.
[36] P. Fernández-Ibáñez, J. Blanco, S. Malato, F.J. de las Nieves, Water Res. 37 (2003) 3180–3188.
[37] G. Li, L. Lv, H. Fan, J. Ma, Y. Li, Y. Wan, X.S. Zhao, J. Colloid Interface Sci. 348 (2010) 342–347.
[38] R.A. French, A.R. Jacobson, B. Kim, S.L. Isley, R. Lee Penn, P.C. Baveye, Environ. Sci. Technol. 43 (2009) 1354–1359.